

# Corrugated Tabs for Supersonic Jet Control

B. Chiranjeevi Phanindra\* and E. Rathakrishnan†

*Indian Institute of Technology Kanpur, Kanpur 208 016, India*

DOI: 10.2514/1.44896

The efficiency of corrugated tabs in promoting the mixing of Mach 1.8 axisymmetric jet has been investigated experimentally. Two rectangular tabs of 4.2% blockage, with corrugations at the edges, located diametrically opposite at the exit of a Mach 1.8 convergent-divergent nozzle were found to be better mixing promoters than identical rectangular tabs without corrugations, at overexpanded, correctly expanded, and underexpanded states of the jet. Furthermore, the corrugated tabs were found to be more efficient in weakening the shocks in jet core compared with the plain tabs. As high as 78% of reduction in core length was achieved with corrugated tabs for the jet operated at nozzle pressure ratio of 7, the corresponding reduction with the plain tabs is only 54%. The mixing effectiveness of corrugated tabs increases progressively with increase of nozzle pressure ratio whereas, the maximum mixing effectiveness of the plain tabs is found to be at the correctly expanded state. The shadowgraph pictures for the uncontrolled and controlled jets clearly demonstrate the effectiveness of corrugated tabs in weakening the waves in the jet core. The speculation of smaller vortices generated by the corrugated tab is supported by a preliminary visualization with water flow channel.

## Nomenclature

$D$	=	nozzle exit diameter
$L$	=	supersonic core length of the jet
$M$	=	Mach number
NPR	=	nozzle pressure ratio
$P_a$	=	atmospheric pressure
$P_b$	=	backpressure
$P_c$	=	pitot pressure
$P_e$	=	nozzle exit pressure
$P_0$	=	setting chamber pressure
$R$	=	distance along the radial direction for uncontrolled jets
$X$	=	axial distance along the $x$ -axis
$x$	=	coordinate along jet axis
$Y$	=	distance along the $y$ -axis (normal to the tabs)
$y$	=	coordinate normal to the tabs
$Z$	=	distance along the $z$ -axis
$z$	=	coordinate along the tabs
$\Delta L$	=	reduction in core length

## I. Introduction

CONTROL of high speed jets with passive control in the form of tabs of various shapes has been reported by large number of researchers in open literature. A tab is essentially a small solid strip kept normal to the flow, usually at the nozzle exit. A tab (strip normal to the flow) generates a pair of counter-rotating transverse vortices (with the axis of rotation along the tab), which become streamwise soon after shedding, that can affect the jet flow development significantly. Smaller the size of vortex better is its mixing promotion efficiency. Also, small vortices are highly stable and can travel longer distances compared with large vortices. The generation mechanism of the streamwise vortex pairs by tabs and their effect on entrainment and spreading of free jets have been discussed in literature [1–3]. In the studies reported so far, tabs of straight edges only have been studied. Recently, it has been demonstrated that the vortex generated by the flat plate can be manipulated to become

smaller by giving a curvature to the plate (Takama [4]). Exploiting this effect, Thanigaiarasu et al. [5] studied arc tabs for jet control. They found that the arc tab is a better mixing promoter than a rectangular tab of equivalent projected area. The reason for this increased mixing efficiency is reported to be the smaller size of the vortices shed by the arc tab. To exploit the advantage of smaller vortices, rectangular tabs with corrugated edges have been studied in the present investigation. To understand the effectiveness of corrugated tabs and their relative superiority compared with identical plain rectangular tabs, jets from a Mach 1.8 axisymmetric convergent-divergent nozzle without control, controlled with corrugated tabs and plain tabs have been investigated both quantitatively and qualitatively in the present study. Measurements of centerline pitot pressure decay, pitot pressure profiles along and normal to the tabs at different axial locations from the nozzle exit, have been carried out over a range of nozzle pressure ratio, covering overexpanded, correctly expanded, and underexpanded states, i.e., the performance of the tabs has been studied in the presence of adverse pressure gradient, zero pressure gradient, and favorable pressure gradient. In addition to the pressure measurements, the supersonic jet field with and without control has been visualized using shadowgraph technique. Preliminary water flow visualization has also been carried out to demonstrate that the vortices generated by the corrugated tab is smaller than those shed by the plain tab.

Bradbury and Khadem [6] were the first to document the effect of tabs in a low-speed jet. With square tabs placed normal to the flow at the nozzle exit, they observed a significant increase in the centerline velocity decay caused by the tabs. It would be fair to say that the flow mechanism responsible for the effect of the tab was far from clear when the investigation was started. Ahuja and Brown [1] reported that for a round jet flow of Mach number 1.12 and total temperature 664 K, the potential core length of the jet could be reduced from about six diameters to less than two diameters by using two diametrically opposed mechanical tabs. They found that the mixing enhancement produced by the two mechanical tabs can reduce the temperature along the jet centerline from 655 K to about 472 K at a distance of five jet diameters downstream, and the mechanical tabs can reduce low-frequency noise by up to 5 or 6 dB. Not until 1993, based on the flow visualization of laser sheet and cigar smoke illumination and pressure measurement of a jet flow, did Zaman [7] propose that the distortion introduced by a mechanical tab is due to a pair of streamwise vortices and which must be responsible for the phenomenal entrainment. It was found that the tabs can distort the jet cross section and increase the jet spread significantly. Subsequent researchers (Bohl and Foss [2], Wishart et al. [8], Zaman et al. [3]) have clearly determined that the tab produces a pair of counter-rotating streamwise vortices. The sense of rotation of the vortex pair is such that fluid from the center of the tab

Received 13 April 2009; revision received 25 July 2009; accepted for publication 3 Sept. 2009. Copyright © 2009 by the American Institute of Aeronautics and Astronautics, Inc. All rights reserved. Copies of this paper may be made for personal or internal use, on condition that the copier pay the \$10.00 per-copy fee to the Copyright Clearance Center, Inc., 222 Rosewood Drive, Danvers, MA 01923; include the code 0001-1452/10 and \$10.00 in correspondence with the CCC.

\*Post Graduate Student, Department of Aerospace Engineering.

†Professor, Fellow of Royal Aeronautical Society, Department of Aerospace Engineering.

base flows toward its tip. The relative magnitude of the peak streamwise vorticity was found to be about 20% of that of the peak azimuthal vorticity for a tabbed circular jet at a Mach number of 0.3 (Zaman [7]). Zaman [7] and Zaman et al. [3] surmised two possible sources of streamwise vorticity for the flow over a tab (Bohl and Foss [2]). The dominant source comes from the pressure hill formed upstream of the tab. The flow deceleration by the tab creates a pressure hill, which together with the presence of the wall, produces the pair of counter-rotating streamwise vortices. The secondary source, again owing to the pressure gradients on the tab surface, is the vorticity shed from the sides of the tab. Initially, vorticity is shed parallel to the edge; as it proceeds downstream, it becomes reoriented by the velocity gradients in the shear layer. Thus, if the tab is tilted downstream, vorticity from primary and secondary sources add together, improving the tab effectiveness (Zaman et al. [3]). In addition to the pressure gradients which flux streamwise vorticity into the flow, the well known necklace or horseshoe vortices due to boundary layer reorientation can also be important in the flow over a tab. Several researchers (Bohl and Foss [2], Reeder and Samimy [9]) have detected the cores of necklace vortices. It should be noted that the sense of rotation of the vortex pair from the pressure hill is always opposite to that of the necklace vortex pair. Since then several studies have reported results with variations in flowfield conditions, as well as tab shape, size, number and angle.

Several other observations regarding optimal tab placement and shape have been made. Reeder and Samimy [9] found that the tab is best placed at the trailing edge. Upstream or detached settings interfere with the pressure hill source of vorticity. Also, the tab height must exceed the boundary layer thickness to generate streamwise vorticity effectively. However, tabs with a much smaller height can produce noticeable effects. In a chemically reacting, compressible, two-stream shear layer, Urban et al. [10] observed a significant increase in product formation and thickening of the shear layer when a tab with a height of only 5% of the boundary layer displacement thickness was placed at the trailing edge. After brief parametric studies, both Zaman et al. [3] and Urban et al. [10] found the optimal tab shape to be triangular. In the usage of Zaman et al. [3], the base of the tab was attached to the exit edge of a nozzle and the apex tilted downstream. This configuration not only worked as effectively as a square tab placed normal to the flow but also incurred less thrust penalty. Navinkumar and Rathakrishnan [11] investigated on the findings of Zaman et al. [7] that for the same projected area, width of the tab is more effective in enhancing the mixing than its length. They found that for the same projected area, length of the tabs is more effective in enhancing the mixing than its width. In addition to the influence of tab geometry on mixing, they had postulated that when the streamwise vortices are introduced right up to the jet centerline it may prove to be an advantage in enhancing the mixing as high as 80%. Further work was done by Sreejith and Rathakrishnan [12] based on the preceding postulation. Instead of tabs, a wire running across a diameter (cross wire) was used as a passive control to enhance the jet mixing. The streamwise vortices introduced by the cross wire lead to a more rapid decay of the centerline pitot pressure. Also, the cross wire was found to weaken the shocks in the jet core significantly. This passive control found to be effective at all levels of expansion. As high as 50% reduction in core length was achieved for Mach 1.79 jet at NPR 5.66. The authors had authentically proved that the limit for tab length is the nozzle exit radius and not the boundary layer thickness. This limit of tab length is termed as Rathakrishnan limit (Lovaraju et al. [13], Mrinal et al. [14]). Most of the studies cited in the foregoing were conducted in free jets discharging into quiescent surroundings. Ahuja [15] and Carletti et al. [16] investigated the effect of tabs for a circular jet with a cylindrical ejector surrounding the jet. Both found an increased mixing within the ejector under the influence of the tabs. Whereas most of the investigations on the effect of tabs have been conducted experimentally, there have also been a few numerical studies (Grosch et al. [17], Steffen et al. [18]). Steffen et al. [18] compared numerical results with corresponding experimental results and noted good agreement in terms of the vorticity field as well as overall jet entrainment. These results lent further credence to the postulations

made on the basic flow dynamics as discussed earlier. Thus it is evident from the preceding discussions that manipulation of the size of the vortices shed by the tabs play a dominant role in promoting the mixing of free jets. Also, it is well known that smaller the size the better its mixing efficiency. With this in mind corrugations were provided at the edges of rectangular tab with the intention to making the tabs to shed smaller vortices, compared with an identical tab without corrugation. The effect of these vortices of reduced size on the mixing enhancement of free jet flow has been demonstrated on a Mach 1.8 jet.

## II. Experimental setup and procedure

The experiments were conducted in the open jet facility at the high speed aerodynamics laboratory, Indian Institute of Technology Kanpur, India. The test facility consists of air supply system (which consists of compressor and storage tanks) and an open jet test facility.

The test facility used consists of a settling chamber, with a provision to mount the jet nozzles on its end plate. The settling chamber is fed with compressed dry air at high pressure (up to 300 psi) through a pressure regulating valve which controls the settling chamber pressure at any desired level before expansion through the jet nozzles.

Pressures were measured with a 16 channel Pressure Systems, Inc., 9010 transducer with a range 0 to 300 psi. The software provided by the manufacturer, was used to interface the transducer with a computer. The user-friendly menu-driven software acquires data, and shows the pressure reading from all the 16 channels simultaneously in a window type display on the computer screen. The software can be used to choose the units of pressure from a list of available units, perform a rezero/full calibration, etc. The transducer also has a facility to choose the number of samples to be averaged, by means of dip-switch settings. The accuracy of the transducer (after rezero calibration) is specified to be  $\pm 0.15\%$  full scale [19]. The pitot pressures were the mean values of pressure averaged over 250 samples per second. This is done because the jet is essentially a turbulent flow which is unsteady. However, the frequency and amplitude of the unsteadiness were not measured because the aim of the present investigation is to compare the mixing effectiveness of corrugated tabs with plain tabs of identical blockage. The repeatability of pressure measurements was  $\pm 3\%$ , respectively.

The pitot probe used was of outer diameter 0.6 mm and inner diameter 0.4 mm. Thus, the ratio of nozzle exit to the probe is  $(13/0.6)^2 = 469.5$ , which is well above the limit of 64 for regarding the probe blockage negligible. The pitot probe was mounted on a rigid 3-D traverse with a resolution of  $\pm 0.1$  mm in linear translation. In all measurements the sensing probe stem was kept normal to the jet axis with its sensing hole facing the flow. The pitot pressures measured were accurate within  $\pm 2\%$ . The pressures measured by pitot probes are significantly influenced by very low Reynolds numbers based on the probe diameter. However, this effect is seldom a problem in supersonic streams because a probe of reasonable size will usually have a Reynolds number above 500, which is above the range of troublesome Reynolds number [20]. For the present probe of outer diameter 0.6 mm, the Reynolds number at NPRs 4 and 8 are 30880 and 61786, respectively. Hence the viscous effect will not cause any error in the pitot pressure measurements.

The experimental model used in the present investigation is Mach 1.8 axisymmetric convergent-divergent nozzle of semidivergence angle 7 deg, made of brass. The exit diameter of the nozzle is 13 mm. The Reynolds numbers of the Mach 1.8 jet coming out of the nozzle, based on nozzle exit diameter, are  $6.6 \times 10^6$  and  $1.34 \times 10^6$ , respectively, for the minimum and maximum NPRs of 4 and 8 of the present investigation. The tabs were made of 1 mm thick aluminum sheet. Two plain rectangular tabs of length 4 mm and width 0.7 mm offering a blockage of 4.2% and two rectangular tabs of identical blockage with corrugation, as shown in Fig. 1 and 2, were used in the present investigation. These tabs were located diametrically opposite at the nozzle exit, as shown in Fig. 1. Recently, Lovaraju et al. [13] showed that the momentum thrust loss suffered due to a cross wire is approximately equal to the projected area of the wire. Also, it is

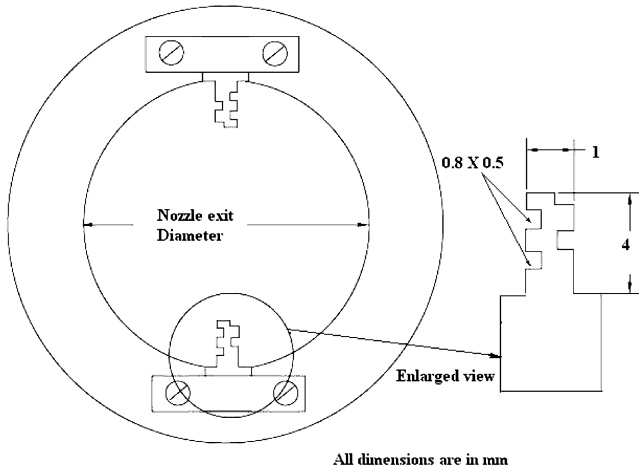


Fig. 1 Sketch of nozzle exit with attached corrugated tabs.

essential to realize that in addition to momentum thrust loss, there is penalty in the form of increased base drag. Thus, the corrugated tabs offering a blockage of 4.2% will cause a momentum loss of around 4.2%.

The centerline pitot pressure distribution, the pitot pressure variation along the tab direction and normal to the tab direction for the controlled jet, and along the radial direction for uncontrolled jet were measured for nozzle pressure ratios 4, 5, 5.74, 6, 7, and 8, covering the overexpanded, correctly expanded, and underexpanded states for the Mach 1.8 jet. In all the three directions, the pitot pressures were measured at intervals of 1 mm, with an accuracy of  $\pm 0.1$  mm. During the measurements the stagnation temperature of the air was approximately 30. The variation in stagnation temperature was  $\pm 0.5$ .

The waves prevailing in the supersonic jet core were visualized using a shadowgraph system with a helium spark arc light source in conjunction with a concave mirror. The shadowgraph images were recorded using a still camera.

A water flow channel was used to demonstrate that the vortices shed from the corrugated rectangular tab are smaller than those shed from the plain rectangular tab. Water flow channel of test-section width 300 mm and water stream depth 5 mm was used for this visualization. For this visualization, the tabs used were different from those used in the jet study. Two rectangular tabs of 1 mm thickness and identical blockage, one without corrugation and other with corrugation were made for this visualization. These tabs were placed in the water flow channel test section which has been tested for uniform flow by using a dye. When there is no model, the dye streaks exhibit a fairly uniform pattern in the test section. The tabs were

placed in the test section at a Reynolds number of 2238 (based on tab width) and the flowfield around the tab and the wake behind the tab were recorded using a video camera. Image of the required portion of flowfield was extracted from the video.

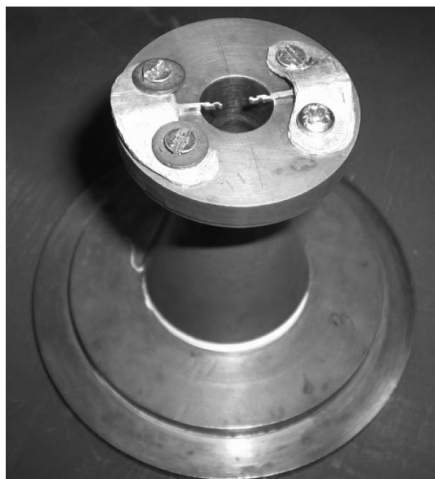
### III. Results and Discussion

#### A. Centerline Pitot Pressure Decay

The centerline pitot pressure decay is an authentic measure of jet propagation (Lovaraju and Rathakrishnan [21]) that is, faster the decay, the faster is the jet mixing with the entrained fluid mass and so on. In other words, the jet centerline pitot pressure decay is a measure of jet mixing; indicating the mixing of the ambient fluid mass entrained at the jet boundary with the mass of the fluid inside the jet [19]. The centerline pressure decay can clearly show the extent of jet core, which is defined as the axial extent up to which the nozzle exit velocity prevails for subsonic jets and the axial extent up to which supersonic flow prevails for supersonic jets. In other words, it can be stated that the core of a jet, either subsonic or supersonic is the distance from nozzle exit at which the characteristic decay begins [19]. The centerline pitot pressure decay for the uncontrolled jet, controlled jet with plain tabs and controlled jet with corrugated tabs are given in Figs. 3–8. At NPR 4, the Mach 1.8 jet is overexpanded with overexpansion ratio  $P_e/P_a = 0.696$ . For this level of expansion, there will be an oblique shock at the nozzle exit to increase the pressure to come to equilibrium with the back pressure, which is the pressure of the atmosphere to which the jet is discharged. The oblique shock from the opposite edges of nozzle exit would cross each other at a distance downstream of nozzle exit. For the present case of axisymmetric nozzle, this shock crossover point would be at the jet axis, which is also the nozzle axis. After crossing over, the oblique shock would get reflected from barrel shock as expansion waves, because reflection from a free boundary is unlike (opposite in nature). These expansion waves would travel up to the opposite boundary of the jet and get reflected as compression waves and these waves travel from one boundary to another boundary and reflect as expansion waves. Thus, there are a large number of compression and expansion waves prevailing in the near field of the jet, where the flow Mach number is supersonic. It is essential to realize that the flow Mach number downstream of the oblique shocks at nozzle exit would be supersonic but with a magnitude less than the Mach number upstream of the shock. This is because all the naturally occurring oblique shocks are weak shocks (Rathakrishnan [22]). Thus, along the jet axis, the flow passes through number of compression waves crossover points and expansion waves crossover points. It is well known that the pressure measured by a pitot probe will decrease with increase in Mach number. As seen in Fig. 3, for the uncontrolled jet, the pitot pressure decreases over a very narrow range of  $X/D$  from 0 to about 0.5. This is because, at the exit of the nozzle, there is an



a) Plain tabs



b) Corrugated tabs

Fig. 2 Photographic view of the tabs attachment: a) plain, and b) corrugated.

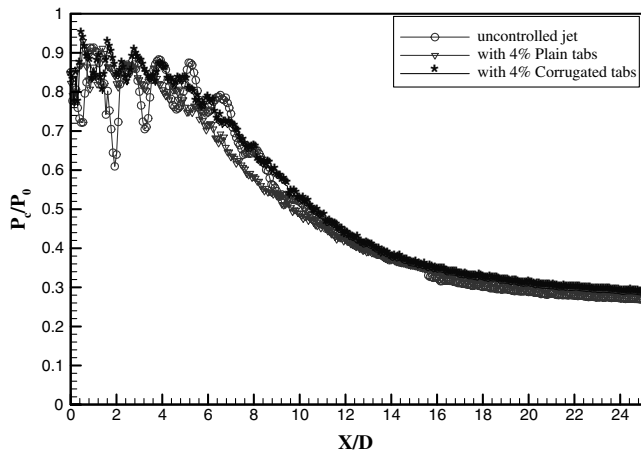


Fig. 3 Centerline pressure decay of jet at NPR 4.

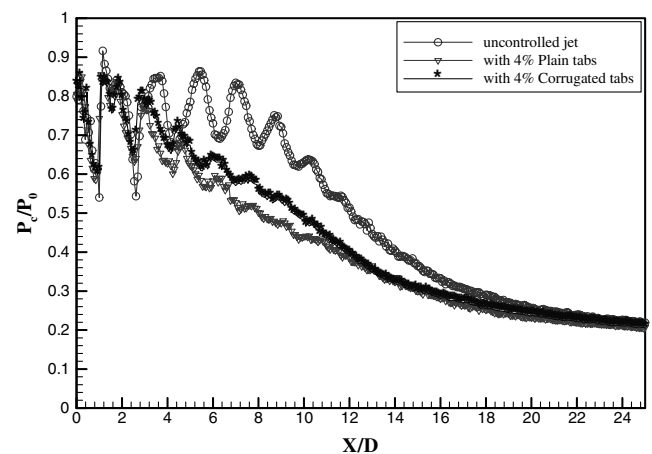


Fig. 6 Centerline pressure decay of jet at NPR 6.

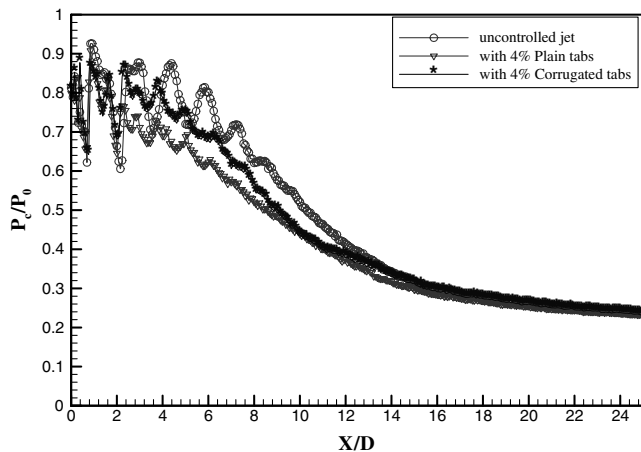


Fig. 4 Centerline pressure decay of jet at NPR 5.

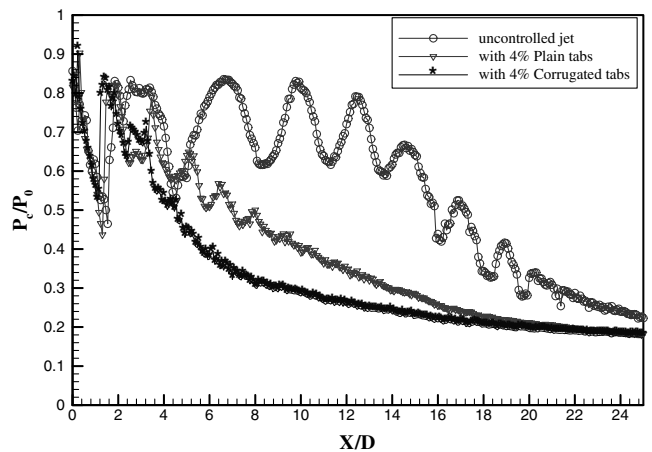


Fig. 7 Centerline pressure decay of jet at NPR 7.

oblique shock caused by overexpansion and an expansion fan caused by the relaxation effect due to the larger space available for the flow to expand soon after exiting the nozzle (Rathakrishnan [23]). Therefore, the combined effect of the compression caused by the oblique shock and the expansion caused by relaxation dictates the flow Mach number. From  $X/D = 0$  to about 0.5, the pitot pressure decrease indicates acceleration of the flow. The pitot pressure attains a minimum at  $X/D = 0.5$ . This should be the location just downstream of shock crossover point, where the flow experiences deceleration due to combined effect of two waves crossing. The flow behind the crossover point essentially becomes subsonic, as it moves downstream. The subsonic flow acceleration as indicated by increase

of pitot pressure from  $X/D = 0.5$  onward. At about  $X/D = 1$ , the flow attains transonic level, followed by acceleration to supersonic Mach numbers. The first pressure maximum peak is a location of transonic Mach number. It is important to note that the subsonic flow downstream of shock crossover point accelerates to higher Mach numbers by gaining momentum from the higher momentum fluid mass around the jet axis, where the flow was traversed by only one compression wave. After attaining the transonic Mach number, the flow encounters acceleration due to momentum gain as well as because of being traversed by expansion waves, which are the reflections of compression waves from the jet boundary. The accelerating flow attains a maximum Mach number at the location, in

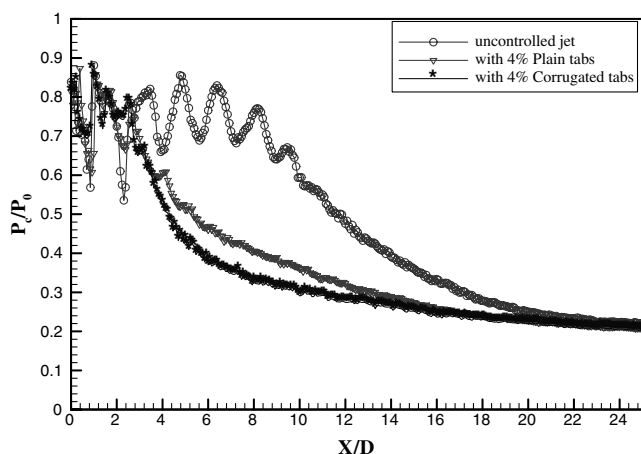


Fig. 5 Centerline pressure decay of jet at NPR 5.74.

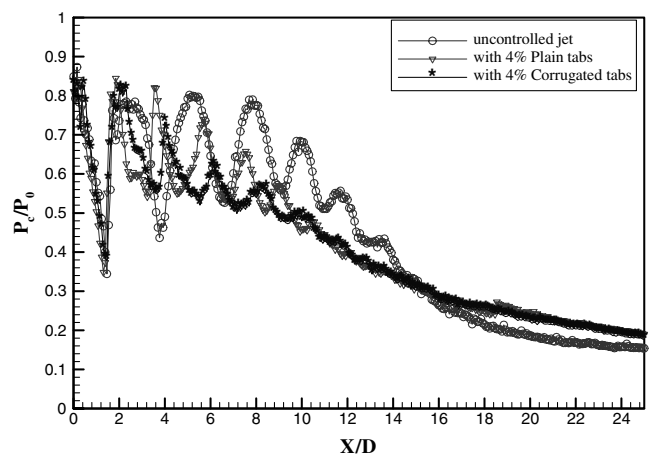


Fig. 8 Centerline pressure decay of jet at NPR 8.

which the pitot pressure shows minimum peak at  $X/D$  slightly less than 2. Downstream of this minimum pressure point, flow accelerates again, attains transonic Mach number, and continues to accelerate to attain a third supersonic Mach number, which is at about  $X/D = 3.2$ . This cycle of acceleration continues exhibiting wavy nature of pitot pressure up to about  $X/D = 8.4$ . Beyond that, there is a continuous decrease of pitot pressure indicating the jet is undergoing characteristic decay. Beyond  $X/D$  about 14, the pitot pressure asymptotically approaches fully developed region. Thus, for the uncontrolled jet, the supersonic core (axial extent up to which wavy nature of supersonic flow prevails) extends to about  $X/D = 8.4$ . From  $X/D = 8.4$  to 14, the flow exhibits characteristic decay, and  $X/D$  beyond 14 could be taken as fully developed zone. The distance between one minimum peak to another minimum peak can be taken as a shock cell length (Lovaraju and Rathakrishnan [21]). Thus, there are about six shock cells for the uncontrolled jet at NPR 4, also the shocks in the jet core are of considerable strength. When the plain tab is placed at the nozzle exit, as expected, the waves in the jet core become weaker, also the core length comes down from  $X/D = 8.4$  for the plain jet, to about  $X/D = 6.4$  for the jet with plain tabs, and to about  $X/D = 6$  for corrugated tab of same blockage of 4.2% as the plain tab. At NPR 4, both plain and corrugated tabs influence the jet mixing significantly, making the waves in the jet core to become weaker compared with the uncontrolled jet.

Centerline pitot pressure decays of the uncontrolled and controlled jets, at NPR 5, are compared in Fig. 4. For this NPR also the jet is overexpanded. But, the overexpansion level comes down from  $P_e/P_a = 0.696$  for NPR 4 to  $P_e/P_a = 0.87$  for NPR 5. In other words, the adverse pressure gradient for NPR 5 is lower than that for NPR 4. For the plain jet, the core extends up to about  $X/D = 8.5$ , the waves present in the core are of considerable strength. For the plain tabs the core length is about  $6D$ ; whereas for the corrugated tabs the core length is about  $5.2D$ . For both the tabs, the waves in the jet core are weaker than the uncontrolled jet. Furthermore, the characteristic decays for the uncontrolled and controlled jets with plain and corrugated tabs are distinctly different.

For the correctly expanded jet at NPR 5.74, as seen in Fig. 5, the tabs could able to bring down the core length from about  $10D$  to  $4D$  for the plain tabs and  $3D$  for the corrugated tabs. That is, a reduction of about 70% in core length is achieved with the corrugated tabs. That is, even in the presence of zero pressure gradient at the nozzle exit, the corrugated tabs could able to promote mixing to a greater extent than the plain tabs. Also the mixing efficiency of the corrugated tabs is much superior to the plain tabs which cause a core length reduction of only about 60%. The characteristic decay for the corrugated tabs is found to be faster than the plain tabs, but in the flowfield beyond  $X/D = 14$  both the tabs influence the field almost identically. This is because, even though the nozzle is correctly expanded, the flow exiting the nozzle finds larger area to relax. This would cause the flow to encounter an associated expansion fan. Because of this, expansion fan at the nozzle exit and the flow accelerates to a higher Mach number downstream of the nozzle exit, and the expansion waves getting reflected as compression waves from the jet boundary coalesce to form shock at the jet axis, and the shock gets reflected as expansion fan and the cycle repeats. Because of this, in the uncontrolled jet, the initial shocks are weaker compared with some of the downstream shocks. But when the tabs are introduced, the shock envelope in front of the tabs results in significant reduction in total pressure and hence a much lower pressure at  $X/D = 0$  compared with the plain nozzle jet. The shocks were found to be very weak for both corrugated and plain tabs. But the core length reductions caused by the plain and corrugated tabs are  $6D$  and  $7D$ , respectively. This is because the mixing promoting small vortices shed by the corrugated tabs are smaller than those shed by the plain tabs. Also, the vortices shed by the corrugated tabs are of variable size, whereas those shed by the plain tabs are of uniform size. Because of the variable size of the vortices, the mixing enhancement achieved with the corrugated tabs is better than the plain tabs. Furthermore, the vortices at the correctly expanded condition find more residential time for interaction with the neighboring vortices, thus resulting in better mixing compared with under and overexpanded conditions. Another

observation can be made based on the nozzle geometry. The present nozzle is a straight convergent-divergent nozzle with a semidivergent angle of 7 deg. Therefore, the flow experiences some divergence (even though mild) owing to the nozzle shape. Therefore, the flow from this nozzle can be expected to experience to better relaxation compared with a contoured or Laval nozzle. Thus the nozzle geometry might cause a marginal difference between the mixing efficiency of the corrugated tabs. But this difference will be insignificant as long as the divergence angle is small, because the relaxation due to availability of larger space at the nozzle exit is predominant. Another parameter, though not considered in the present study, which would be of great value is the penetration of the corrugated tabs in to the jet, i.e., the tab length variation for a given blockage.

As seen from Fig. 6, at NPR 6, which is with marginal favorable pressure gradient at the nozzle exit, the core length for uncontrolled jet extends up to about  $11.4D$ , whereas for the jet from nozzle with plain tabs the core length comes down to about  $9.2D$ , and with corrugated tabs the core length comes down to  $8.4D$ . That is, the plain tabs reduce the core length to about 19% and the corrugated tabs reduce the core length to about 26%. Also, the waves in the first three shock cells are weaker for the corrugated tabs than the plain tabs.

At NPR 7, as seen from Fig. 7, the waves in the core of the uncontrolled jet become very strong, and the core extends as long as about  $20D$ . For the plain tabs, the core comes down to about  $9.2D$ . Also, the waves in the core beyond the first shock cell are made significantly weaker. The corrugated tabs result in a drastic reduction of jet core to about  $4.4D$ . This is about 78% decrease in the core length. Another interesting fact is that the shocks in the core, including the first cell are made considerably weaker by the corrugated tabs. The difference in the area enclosed by pitot pressure curve is larger for the corrugated tabs, indicating the mixing provided by corrugated tabs is much larger than the plain tabs. For this case, the jets with tabs show their individual identity up to about  $18D$ .

At the largest tested NPR of 8, the favorable pressure gradient is  $P_e/P_a = 1.392$ . The results shown in Fig. 8, show that the core length for uncontrolled jet extends to about  $13.6D$ , whereas for the jet from nozzle with plain tabs, the core length comes down to about  $12.8D$  and for the jet from nozzle with corrugated tabs, the core length comes down to about  $11.2D$ . Even though the core length achieved with corrugated tabs is not drastic, the corrugated tabs cause the waves in the jet core to become weaker compared with the plain jet. Though acoustic measurements are not made in the present investigation, weakening the waves in jet core can be taken as an advantage from noise reduction point of view (Verma and Rathakrishnan [24]).

From the preceding discussions of centerline pressure decay of uncontrolled and controlled jets, it is evident that the effectiveness of tabs is strongly dictated by the level of expansion at the nozzle exit. An interesting feature found is that, unlike the literature information namely, the control effectiveness increases with increase of favorable pressure gradient, and the tabs are found to be most efficient at and around correctly expanded condition. This kind of observation was also reported by Navinkumar and Rathakrishnan [11] for the limiting case of the tab length namely, a tab running across the diameter of the nozzle exit, named cross wire. Therefore, it is essential to relook into the statement that the control effectiveness increases with increase of favorable pressure gradient as report in the literature.

The core length reduction achieved with the plain tabs and corrugated tabs are calculated for all the NPRs. The percentage reduction in core length is defined as

$$\text{Percentage reduction in core length } (\Delta L) = \frac{(\text{Core})_{\text{uncontrolled jet}} - (\text{Core})_{\text{controlled jet}}}{(\text{Core})_{\text{uncontrolled jet}}} \times 100$$

and also the effectiveness of corrugated tabs over plain tabs is defined as

**Table 1 Core length of the jet at different NPRs**

NPR	Uncontrolled jet, $L$	Jet with plain tabs, $L$	Jet with corrugated tabs, $L$
4	$8.4D$	$6.4D$	$6.0D$
5	$8.4D$	$6.0D$	$5.2D$
5.74	$10.0D$	$4.0D$	$3.0D$
6	$11.4D$	$9.2D$	$8.4D$
7	$20.0D$	$9.2D$	$4.4D$
8	$13.6D$	$12.8D$	$11.2D$

**Table 2 Percentage reduction in core length at different NPRs**

NPR	Percentage reduction in core length of jet with plain tabs	Percentage reduction in core length of jet with corrugated tabs	Effectiveness of corrugated tabs over plain tabs
4	23.81%	28.57%	20.00%
5	28.57%	38.09%	33.33%
5.74	60%	70.00%	16.67%
6	19.30%	26.31%	36.36%
7	54%	78.00%	44.44%
8	5.88%	17.65%	200.00%

$$\text{Effectiveness} = \frac{(\Delta L)_{\text{Corrugated tabs}} - (\Delta L)_{\text{Plain tabs}}}{(\Delta L)_{\text{Plain tabs}}} \times 100$$

where,  $(\Delta L)$  is reduction in core length.

The core length, core length reduction, and the effectiveness of corrugated tabs over plain tabs at different NPRs are tabulated in Tables 1 and 2. The core length variation with NPR for the uncontrolled jet, the core length increases with NPR up to 7 and then comes down drastically at NPR 8. For the plain tabs, the core length shows an oscillatory nature as seen from Fig. 9. For the corrugated tabs also the variation is oscillatory, but, at all levels of expansion (i.e., at all NPRs), the core length of jet from nozzle with corrugated tabs is less than that of the plain tabs (Fig 10). This clearly reveals that the mixing efficiency of corrugated tabs is higher than that of plain tabs at all the three levels of expansion, namely, over expanded, correctly expanded, and underexpanded states. In other words, in the presence of adverse pressure gradient, zero pressure gradient (no pressure gradient), as well as favorable pressure gradient, the corrugated tabs are more efficient in mixing promotion than the plain tabs. However, the effectiveness of corrugated tabs is strongly influenced by the level of expansion, as seen from Fig. 11.

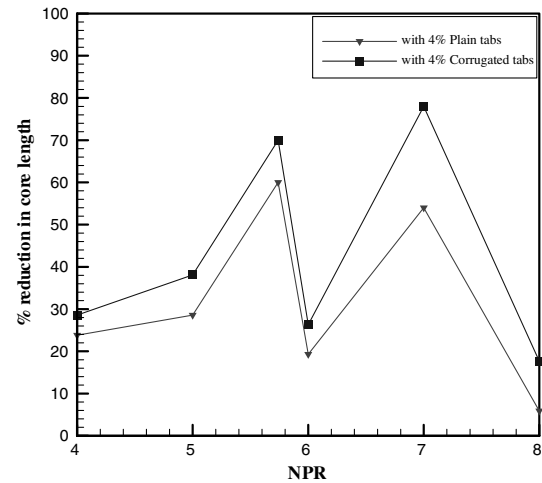
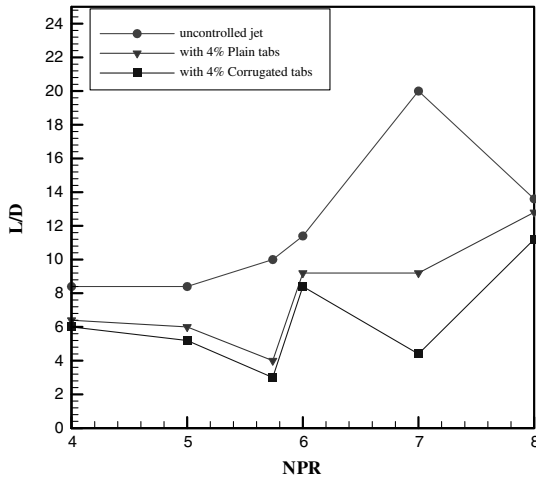
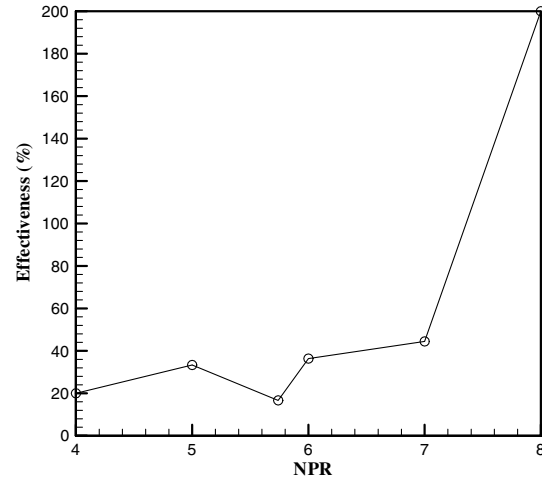
Thus it can be summarized that generation of smaller vortices by the corrugated tabs, compared with uniform size vortices shed by the plain tabs, is more efficient in promoting mixing in accordance with

the vortex dynamics that, smaller the vortex size, the better the mixing efficiency.

## B. Pressure Profiles

The pitot pressure ( $P_c$ ) distribution, measured along the tabs, and normal to the tabs directions for the controlled jets, and along the radial direction for uncontrolled jet, is made nondimensional by dividing with the settling chamber pressure ( $P_0$ ). The radial ( $R$ ) transverse ( $Y$ ), i.e., along the tab and normal ( $Z$ ), i.e., normal to the tab are made nondimensional by dividing them with nozzle exit diameter ( $D$ ).

The pitot pressure profiles for the uncontrolled jet at axial distances of  $X/D = 0.5, 1, 2, 4, 6$ , and  $10$ , are presented in Fig. 12, for NPR 4. At  $X/D = 0.5$  it is seen that, at the jet axis, the pitot pressure is the minimum; this implies that the jet velocity is maximum at that point. Away from the jet axis, the pitot pressure shows almost constant level up to about  $R/D = 0.5$ , followed by a steep decrease from  $0.5$  to  $0.6$ . Beyond  $R/D = 0.6$ , the pitot pressure remains almost a constant with a magnitude of  $P_c/P_0 = 0.25$ . At  $X/D = 1$ , around the axis, the pitot pressure exhibits almost a constant pressure zone. This implies that there is a uniform Mach number zone around the jet axis. This prevails from  $R/D = 0$  to about  $0.3$ . For  $R/D$  greater than  $0.3$ , the pitot pressure decreases sharply up to about  $R/D = 0.6$ . Beyond that, the pressure remains almost the same. At  $X/D = 2$ , the constant pitot pressure magnitude around the jet axis is higher than  $X/D = 1$ . But, the radial extent of this peak pressure is from  $R/D = 0$  to about  $0.25$  only. At  $X/D = 4$ , the pitot pressure peak value comes down to  $0.8$ , and also the decrease of pressure shows a relatively more gradual variation

**Fig. 10 Percentage reduction in core length with NPR.****Fig. 9 Variation of core length with NPR.****Fig. 11 Effectiveness of corrugated tabs over plain tabs.**

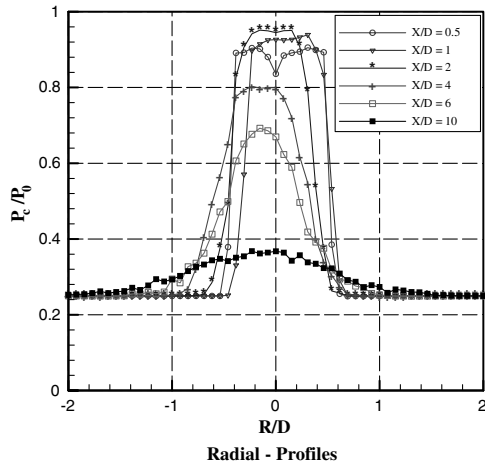


Fig. 12 Pressure profiles for uncontrolled jet at NPR 4.

than the near field profiles upstream of this location. At  $X/D = 6$  there is no constant pressure zone around axis, as exhibited by the single peak pitot pressure profile. Also, in the radial direction pressure decreases gradually, attaining minimum pressure level of  $P_c/P_0 = 0.2$  at  $R/D = \text{around } 1$ . At  $X/D = 10$ , the jet has encountered the characteristic decay and the pitot pressure decay shows almost fully developed nature. In all these profiles it is interesting to note that the pressure profiles are not symmetric about the jet axis. This is because the jet field is essentially vortex dominated and hence, due to the vortex action, the field is rendered

asymmetric, even though the jet delivered by the nozzle at  $X/D = 0$  is essentially axisymmetric. In other words, the azimuthal vortices formed at the nozzle exit and the mass entraining large vortices formed at the jet boundaries have their own frequencies. The azimuthal vortices can be identical in size provided the nozzle exit is absolutely symmetric. But in reality there is bound to be some asymmetry, owing to manufacturing error. Another reason causing the azimuthal vortices formed to become nonuniform is the boundary layer at the inner surface of the nozzle. The combined effect of these marginal variations in the size of the azimuthal vortices and the vortices formed at the jet boundary introduces noticeable asymmetry to the jet in the near field.

For the controlled jet with plain tabs, the pitot pressures along the tab direction ( $z$ -profiles) normal to the tabs ( $y$ -profiles) for NPR 4, at  $X/D = 0.5, 1, 2, 4, 6$ , and  $10$  are shown in Figs. 13a and 13b. It is seen that the  $y$ -profile at  $X/D = 0.5$  does not exhibit any dip as in the case of uncontrolled jet. Further, there is a constant pressure zone around the jet axis. This is a clear indication of the mixing caused by the vortices shed from the tabs right at the nozzle exit. Further, the fall after the peak pressure is also slightly reduced compared with the uncontrolled jet. The jet is rendered more asymmetrical compared with the uncontrolled jet. Another interesting feature is that the pressure profiles at  $X/D = 1, 2$ , and  $4$  are with marginal variation in the peak pressure around the jet axis. This is a clear indication of momentum transport caused by the control tabs. For  $X/D = 6$  the peak pressure is much higher than the uncontrolled jet. This is because the shock cells are made weaker by the tabs, as seen in the centerline pressure decay plots. Because of these weakened waves, the flow could be able to retain its pressure level to a longer distance compared with the uncontrolled jet. Because of similar reason, at

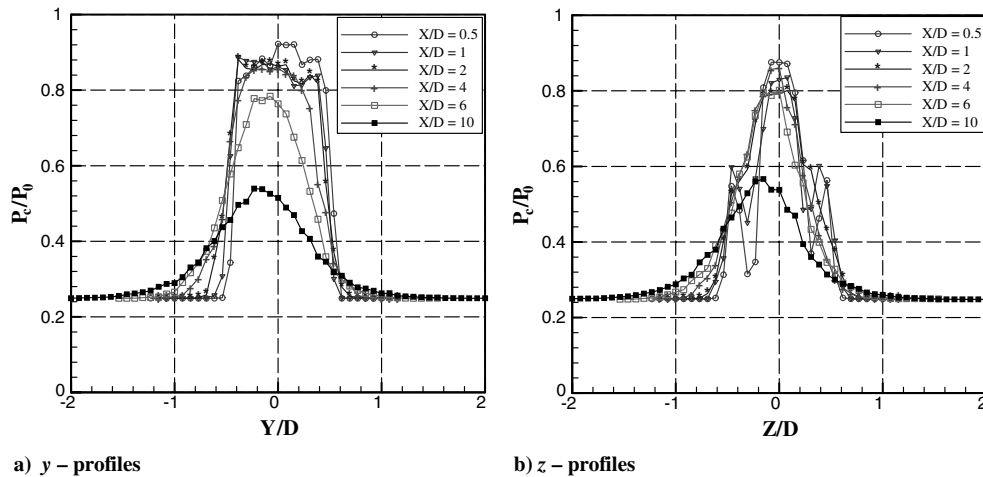


Fig. 13 Pressure profiles for jet with plain tabs at NPR 4: a)  $y$ -profiles, and b)  $z$ -profiles.

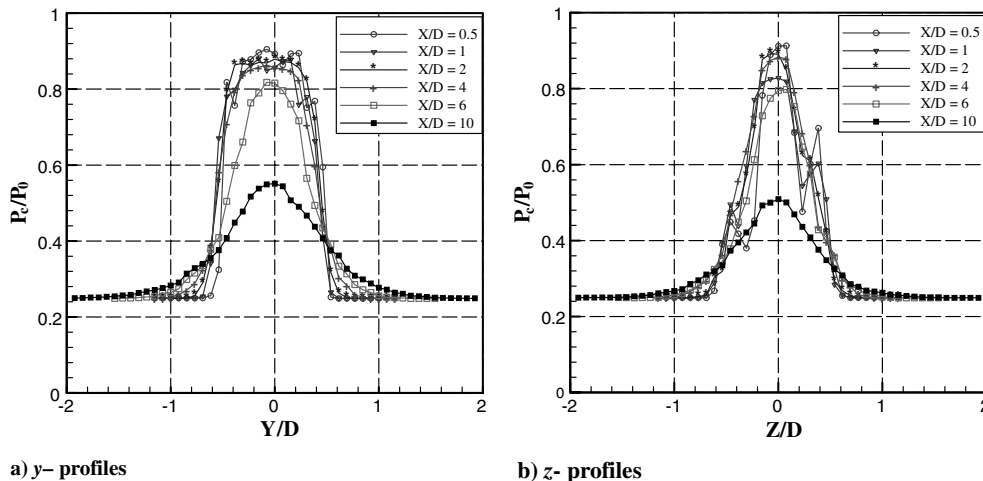


Fig. 14 Pressure profiles for jet with corrugated tabs at NPR 4: a)  $y$ -profiles, and b)  $z$ -profiles.

$X/D = 10$  also, the peak pressure is greatly larger than the uncontrolled jet. However, in the far field the pressure levels are almost comparable to the uncontrolled jet. This feature was observed as almost similar asymptotic decay of controlled and uncontrolled jets in the far field from the centerline pitot pressure decay results. The  $z$ -profiles (Fig. 13b) are distinctly different from the  $y$ -profiles. This is a clear indication of the asymmetry to the jet propagation introduced by the tabs. In  $z$ -profiles, the peak profile zone is narrower at all axial distances compared with the  $y$ -profiles. This is because, in the direction normal to the tabs, the flow could not spread greatly without the influence of the vortices shed by the tabs. In other words, as in the case of the direction along the tab, normal to the tab, the flow could not relax because of the absence of any solid body. In the  $z$ -profiles at about  $X/D = 2, 4$ , and  $6$ , the profiles exhibit off-center peaks. This shows that, slightly downstream of the tabs, the jet is essentially bifurcated exhibiting two high-velocity zones on either side of the jet axis. But at  $X/D = 10$ , the  $z$ -pressure profile is almost identical to that of  $y$ -profile. In the far field,  $z$ -profiles are identically the same as the radial profiles for uncontrolled jets as well as  $y$ -profiles.

The pressure profiles along  $y$ - and  $z$ -directions for the jet with corrugated tabs are shown in Figs. 14a and 14b. It is seen that in the  $y$ -direction, the space between the tabs experiences more uniform flow than the plain tabs. Also, at  $X/D = 1$  and  $2$  the pressure profiles show wider uniform pressure zones compared with the plain tabs. The pressure profile peak at  $X/D = 6$  is higher than that of the plain tabs. These features clearly demonstrate that the mixing caused by the corrugated tabs is much superior to the plain tabs. For corrugated tabs the pressure profiles retain their signature even beyond  $Y/D = 1$ . The  $z$ -profiles, shown in Fig. 14b, exhibit similar features as the plain tabs in the near field. But the off-center peaks show drastically

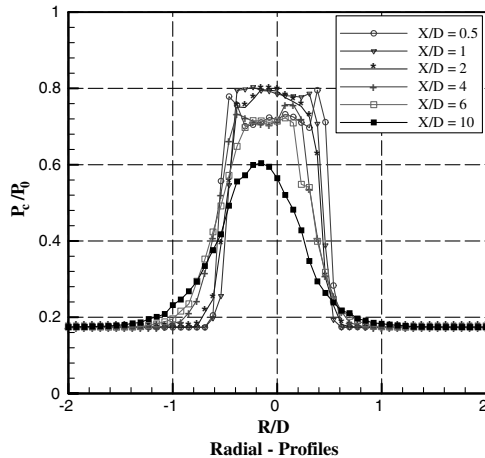
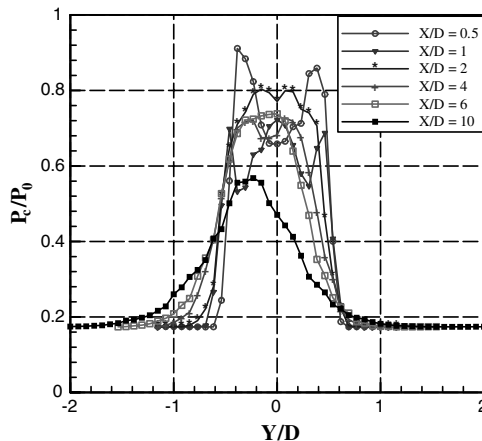
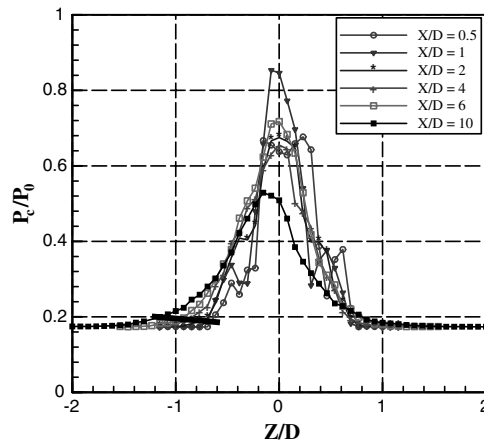


Fig. 15 Pressure profiles for uncontrolled jet at NPR 5.74.



a)  $y$ -profiles



b)  $z$ -profiles

Fig. 16 Pressure profiles for jet with plain tabs at NPR 5.74: a)  $y$ -profiles, and b)  $z$ -profiles.

different magnitudes on either side of the jet axis. Because of this, the mixing beyond the off-center peak locations is bound to become greater than a field with almost identical off-center peaks. Thus, the differential off-center peaks can be regarded as the direct indication of the better mixing caused by the corrugated tabs. The far-field behavior of  $z$ -profile is almost identical to the plain tabs.

The pressure profiles for the correctly expanded jets from nozzle without and with tabs are presented in Figs. 15–17. At NPR 5.74 the jet is correctly expanded with zero pressure gradient at the nozzle exit. Therefore, it might be expected that the pitot pressure profile at  $X/D = 0.5$  is of uniform magnitude over a radial distance from the jet axis.

For correctly expanded Mach 1.8 supersonic flow, the pitot pressure is supposed to read  $P_c/P_0 = 0.8127$ , as per the isentropic theory. But, in the results shown in Fig. 15 at  $X/D = 0.5$ , the  $P_c/P_0$  is around 0.72 over a radial distance around the jet axis followed by a gradual increase reaching about 0.8. This clearly implies that, around the jet axis, the Mach number is higher than 1.8. This is in accordance with the results of Verma and Rathakrishnan [24], which states that a flow, even at correctly expanded condition, encounters an expansion fan at the nozzle exit, due to the relaxation experienced by the flow because of the availability of larger space. Therefore, the flow accelerates to begin with and then encounters the reflected compression waves from the jet boundary. These features are reflected as  $P_c/P_0$  corresponding to Mach number 1.8 around the jet axis, followed by the increase of  $P_c$  (decrease of Mach number). This process is inferred even at  $X/D = 1$ . At  $X/D = 2$  the pressure peak is around the axis, followed by a gradual decrease and a subsequent steep fall. The waves prevailing in the near field for this case are of marginal strength. At  $X/D = 10$ , the pressure profiles show a single peak followed by gradual, but considerable, decay up to  $R/D = 0.5$ . Beyond  $R/D = 0.5$  the decay is asymptotic. For this case also, the pressure profiles for uncontrolled jet exhibits asymmetry as in the case of overexpanded jets. It is interesting to note that the spread of the uncontrolled jet at NPR 5.74 is slightly less than that at NPR 4. This may be because the inertia of the overexpanded jet flow just downstream of the nozzle is less than that of correctly expanded jet because of the oblique shock at the nozzle exit. This would offer more residential time for the azimuthal vortices shed from the nozzle exit to interact with the vortices formed at the jet boundary, leading to better mixing compared with the correctly expanded jet for which the velocity just downstream of the nozzle exit is larger than NPR 4, owing to the expansion fan caused by the relaxation effect.

When the plain tabs are placed at nozzle exit the jet experiences mixing right from the nozzle exit. However, the mixing initiation by the tabs is just in the proximity of the tabs. Because of this, in the near field waves continue to prevail. However, the strength of the waves is greatly reduced by the mixing process initiated by the tabs. At  $X/D = 5$  the minimum pressure dip is lower than the uncontrolled jet. But this cannot be taken as an indication of larger Mach number



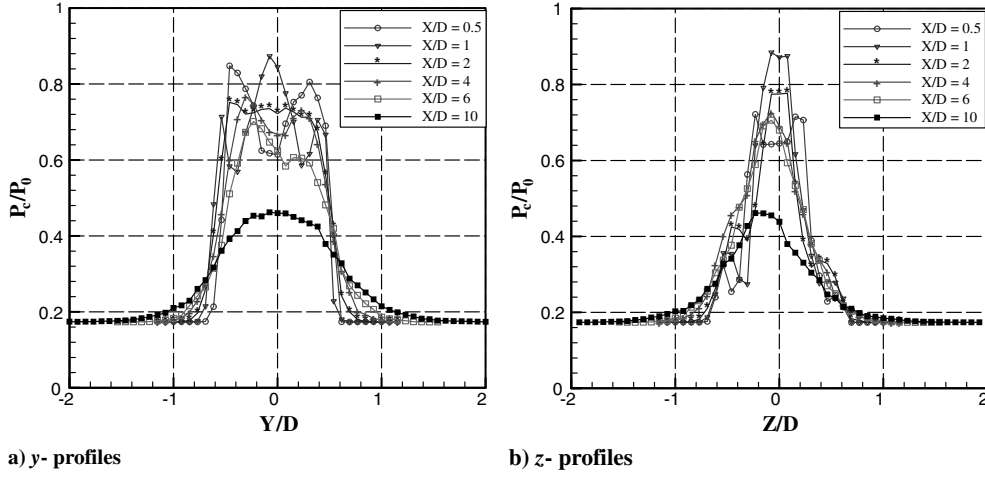


Fig. 17 Pressure profiles for jet with corrugated tabs at NPR 5.74: a) y-profiles, and b) z-profiles.

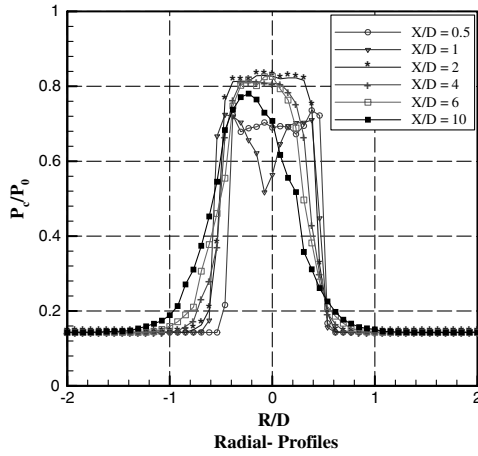


Fig. 18 Pressure profiles for uncontrolled jet at NPR 7.

than the uncontrolled jet. Because the flow encounters severe loss due to the additional shocks caused by the presence of the tabs. The waves at  $X/D = 2$  are found to be much weaker than the uncontrolled jet. This is due to the mixing augmentation caused by the tabs. The asymmetry of the pressure profiles in the y-direction is considerable. The z-profiles shown in Fig. 16b show that the spread in the direction normal to the tabs is less than that in the direction along the tabs. Also, normal to the tabs the jet continues to exhibit asymmetry.

The pressure profiles for corrugated tabs are shown in Figs. 17a and 17b. It is seen that in the near field the waves are seen, but as early

as  $X/D = 2$  the jet spread is greatly larger than the plain tabs. Also, at  $X/D = 10$  the jet momentum is greatly reduced by the efficient mixing caused by the corrugated tabs, compared with the plain tabs. Furthermore, because of efficient mixing the jet asymmetry is greatly reduced as seen in Fig. 17a. In the direction normal to the tabs, as seen from z-profiles in Fig. 17b, the jet spread is considerably larger at  $X/D = 0.5$  and 1, compared with the plain tabs. In this direction also, the jet diffuses faster than the plain tabs, as reflected as the peak pressure value of about 0.46 at  $X/D = 10$ , against 0.58 at the same axial distance for the plain tabs. Thus even in the presence of no pressure gradient, the corrugated tabs perform better than the plain tabs.

At NPR 7, Mach 1.8 jet is considerably underexpanded with a favorable pressure gradient of  $P_e/P_a = 1.218$ . Therefore, the expansion fan at the nozzle exit has to be powerful. Because of this, the Mach number at the nozzle axis in the near field would be much higher than the jet Mach number 1.8.

As seen in Fig. 18, the  $P_c/P_0$  along the axis at  $X/D = 0.5$  is about 0.52, which is very much lower than that for NPR 6. At  $X/D = 1$ , the pressure level is almost identical to NPR 6 around the jet axis, same is the case for  $X/D = 2, 4, 6$ , and 10. But the almost uniform Mach number zone at  $X/D = 1$  and 2 for NPR 7 is much wider than NPR 6. Asymmetry is well pronounced for this underexpanded state also. The pressure profiles for the plain tabs shown in Figs. 19a and 19b reveal that the jet spread at NPR 7 is slightly higher than NPR 6, in both along and normal to the tabs. Also, the waves prevail as far as  $X/D = 6$ ; the asymmetry is also larger than NPR 6.

For the corrugated tabs, as seen in the pressure profiles shown in Figs. 20a and 20b, the jet spread is larger than that of the plain tabs at corresponding NPR. Also, mild waves are observed even at  $X/D = 10$ , this may be because the initial waves are made weaker by

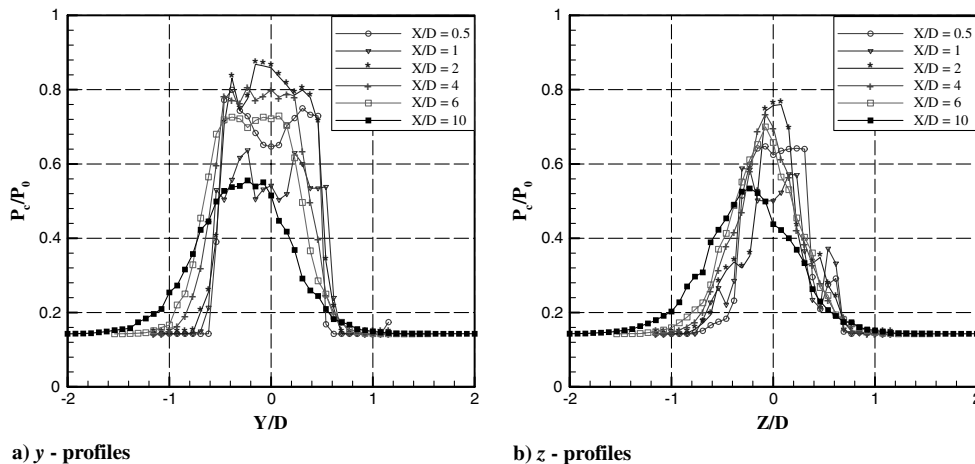


Fig. 19 Pressure profiles for jet with plain tabs at NPR 7: a) y-profiles, and b) z-profiles.

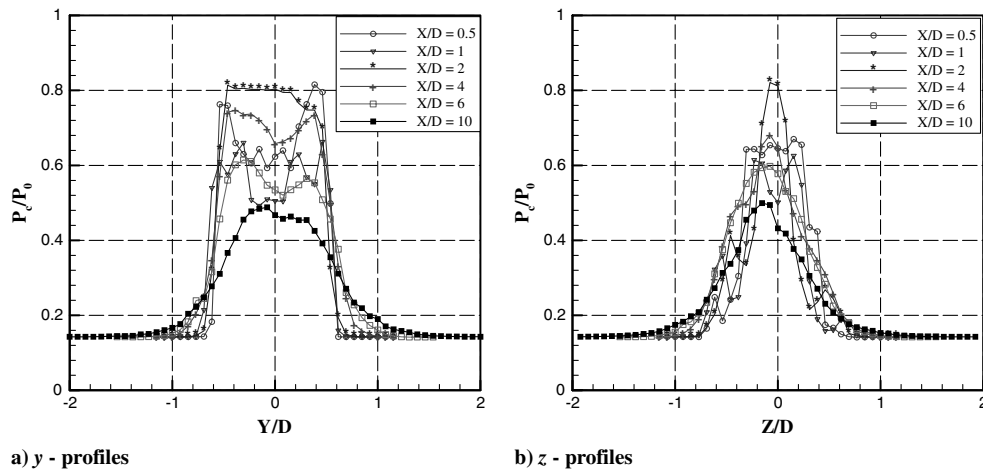


Fig. 20 Pressure profiles for jet with edge corrugated tabs at NPR 7: a) y-profiles, and b) z-profiles.

the corrugated tabs. Therefore, flow traversed by the weaker waves could possess considerable momentum over a longer distance than the field traversed by the initially stronger waves as in the case of plain tabs. Like in the case of lower NPRs, the jet asymmetry is greatly reduced by the corrugated tabs. This once again emphasizes that the mixing caused by the corrugated tabs is superior to the plain tabs.

### C. Optical Flow Visualization

Shadowgraph technique was employed to visualize the waves prevailing in the jet with and without control at different NPRs of the present study. For the controlled jets, visualization carried out viewing along the tabs and normal to the tabs.

At NPR 4, which is an overexpanded state for Mach 1.8 jet, the oblique shocks at the nozzle exit are clearly seen (Fig. 21). These oblique shocks cross each other at the jet axis and reach the barrel shock. On reaching the barrel shock, the oblique shock reflects as expansion fan, because reflection from fluid boundary is unlike (Rathakrishnan [22]). The kink formed at the shock reflection points are clearly seen in the picture. The expansion waves cross each other and reach the boundary and reflect back as compression waves. The reflected compression waves once again cross each other at the jet axis and reflect back as expansion fan from the barrel shock boundary. This kind of wave reflection continues to some downstream distance. The distance between successive shock reflection points (kinks) is called shock cell length. At NPR 4, four cells are noticeable. The first two cells are prominent and third and fourth are weak cells.

For the controlled jets with plain tabs and corrugated tabs, the visualization pictures in the direction normal to the tabs are shown in Fig. 22a for NPR 4. It is interesting to see that the shock cells prevailing in the uncontrolled jet are greatly disturbed resulting in a number of smaller diamond like structures for both plain and corrugated tabs. However, as it can be seen in Fig. 22a, the first diamond for the plain tabs is longer. But the second diamond for the corrugated tabs is larger than that of the plain tabs and it alternates. This kind of number of wave crossings is seen up to some



Fig. 21 Shadowgraph picture for uncontrolled jet at NPR 4.

downstream distance for both the tabs. There are four prominent diamonds along the centerline for the plain tabs. But, for the corrugated tabs only three such diamonds are prominent.

The visualization pictures in the direction along the tabs are shown in Fig. 22b. Compared with normal to the tabs, along the tabs the wave pattern is completely different. Furthermore, the waves in the plain tabs case are relatively stronger than the corrugated tabs.

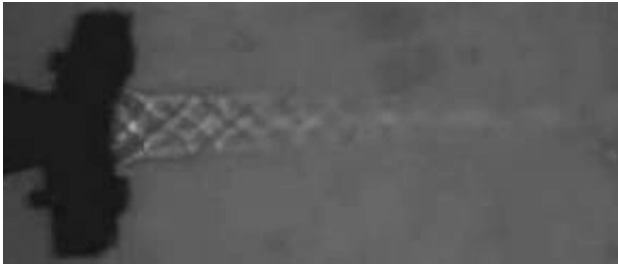
At NPR 5.74, which is the correctly expanded condition for Mach 1.8 jet, the waves prevailing in uncontrolled jet field are shown in Fig. 23. It is interesting to note that, even at the correctly expanded condition, the jet field is wave dominated. This is because, as explained by Rathakrishnan [23], the jet encounters an expansion fan due to the relaxation effect. These expansion waves get reflected as compression waves and the process continues. For this case also, two prominent shock cells are visible.

The waves prevailing in the correctly expanded controlled jet operated at NPR 5.74 are shown in Figs. 24a and 24b. As discussed in the pressure profiles, there are waves in the jet core due to the relaxation effect. For the plain tabs, in the direction normal to the tabs, the waves are seen up to a considerable distance downstream of the nozzle exit. This may be because of the expansion at the exit is not strong, as it is only due to the relaxation effect. Because of this, the flow Mach number changes caused by the waves are not drastic. Owing to this, supersonic nature of jet could be able to prevail over a longer distance compared with NPR 4, which is an overexpanded operation. Along the tabs also, the shock cells prevail over longer distance compared with NPR 4.

At NPR 7 (underexpanded state for the jet) the expansion fan at nozzle exit is stronger. Because of the stronger expansion, the centerline Mach number reaches a much higher value, resulting in longer shock cells. For this case, even the third cell is considerably longer and stronger, as seen in Fig. 25.

At NPR 7, which is considerably highly underexpanded operation, strong waves are visible in the first few cells for the plain tabs in the direction normal to the tabs (Fig. 26a). But for the corrugated tabs, the waves are considerably weaker due to enhanced mixing efficiency of these tabs. In the direction along the tabs, for the plain tabs, even the third cell shows shock crossover point, but for the corrugated tabs, the third cell has only very weak waves. For both plain tabs and corrugated tabs, the jet spread is more in the direction normal to the tabs ( $xy$ -plane) compared with the direction along the tabs ( $xz$ -plane).

The shadowgraph pictures clearly demonstrate the difference in the wave domination in the supersonic core and the effect of additional or augmented mixing of the corrugated tabs compared with the plain tabs. It is well known that shock cell length reduction and weakening of waves in the jet core can be taken as a measure of reduced shock associated noise. Therefore, it can be justifiably stated that even though jet noise has not been measured, the control with corrugated tabs is advantageous for jet noise reduction point of view also.



With Plain tabs



With Corrugated tabs

a) Viewed normal to the tabs,  $xz$ -plane



With Plain tabs



With Corrugated tabs

b) Viewed along the tabs,  $xy$ -plane

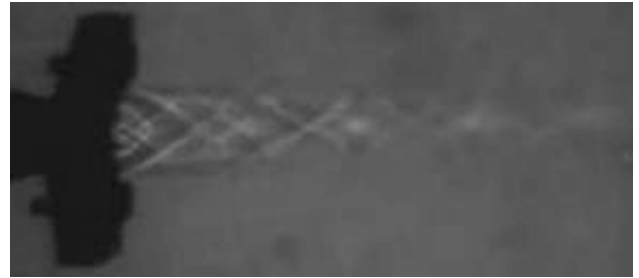
**Fig. 22** Shadowgraph pictures for controlled jet at NPR 4: a) viewed normal to the tabs  $xz$ -plane, and b) viewed along the tabs  $xy$ -plane.

#### D. Water Flow Visualization

It was found that the corrugated tab causes better mixing than the plain tab. The physical reason for this was speculated as the vortices shed from the corrugated tab were relatively smaller than those shed



**Fig. 23** Shadowgraph picture for uncontrolled jet at NPR 5.74.



With Plain tabs



With Corrugated tabs

a) Viewed normal to the tabs,  $xz$ -plane



With Plain tabs



With Corrugated tabs

b) Viewed along the tabs,  $xy$ -plane

**Fig. 24** Shadowgraph pictures for controlled jet at NPR 5.74: a) viewed normal to the tabs  $xz$ -plane, and b) viewed along the tabs  $xy$ -plane.

by the plain tab. To evaluate this speculation, a modest experimental visualization with water stream as the flow medium was conducted. Flow past identical rectangular tabs, one with corrugation and one without corrugation, was visualized. The plain and corrugated tabs

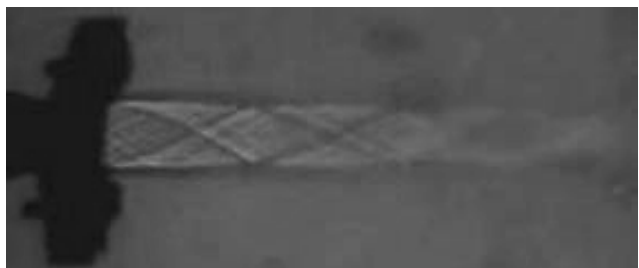


**Fig. 25** Shadowgraph picture for uncontrolled jet at NPR 7.



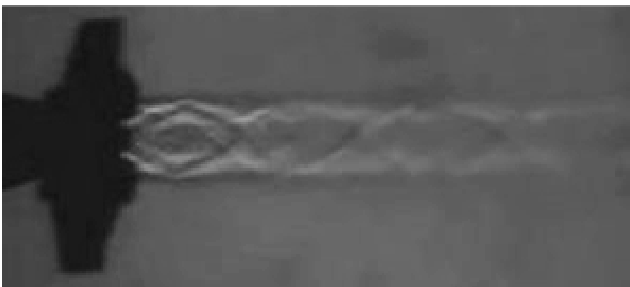
With Plain tabs



With Corrugated tabs

a) Viewed normal to the tabs,  $xy$ -plane

With Plain tabs



With Corrugated tabs

b) Viewed along the tabs,  $xy$ -plane

Fig. 26 Shadowgraph pictures for controlled jet at NPR 7: a) viewed normal the tabs  $xz$ -plane, and b) viewed along the tabs  $xy$ -plane.

were placed in the test section with a water stream speed of 20 cm/sec. By injecting water color dye, the flowfields behind the plain and corrugated tabs were visualized. The two pictures of flowfield around the plain and corrugated tabs are given in Figs. 27a and 27b. It is seen that in the wake of the corrugated tab the vortices are smaller, thus causing a better mixing compared with the plain tab. Furthermore, the flow deviation caused by the plain tab is found to be much larger than the corrugated tab. This is because the vortices leaving the plain tab are of uniform size and larger than those shed by the corrugated tab. Therefore, the vortices shed by the plain tab take some distance and time before they could interact and promote mixing. On the other hand, the vortices shed by the corrugated tabs are of variable size and smaller than the vortices from the plain tab. The varying size of the smaller vortices causes mixing right from the corrugated tab location. This leads to reduced amplitude of the flow deviation compared with the plain tab. It is important to note that these results are only qualitative in nature and meant to get an understanding about the speculation that the smaller the vortices shed by the tab, the better would the mixing caused by them. Another aspect of the corrugation is that it offers better relief to the incoming flow compared with the plain tab, even though both the tabs offer the same blockage. Because of this the flow deviation upstream of the corrugated tab is smaller than the plain tab, as seen in Figs. 27a and 27b. Also, the Reynolds number of water stream, based on the width of the tab, is just 2238. Therefore, these observations cannot be compared with the jet field. However, the corrugated tab shedding smaller vortices can be taken as a supportive evidence of speculation used in the discussion of results of centerline pitot pressure decay and pitot pressure profiles of jets controlled with plain rectangular and corrugated rectangular tab.

#### IV. Conclusions

The quantitative and qualitative results of present investigation clearly demonstrates the following.

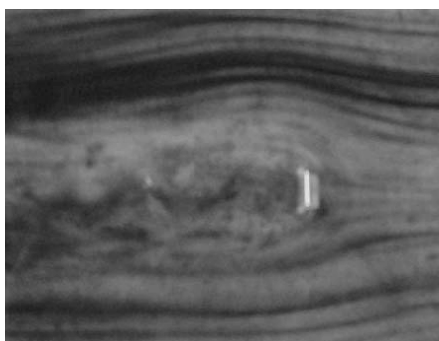
1) The corrugated rectangular tabs are better mixing promoters than identical plain rectangular tabs.

2) As high as 78% of reduction in core length is achieved with corrugated tabs for Mach 1.8 jet operated at NPR 7, which is 24% higher than the core length reduction achieved with plain tabs at the same operating condition.

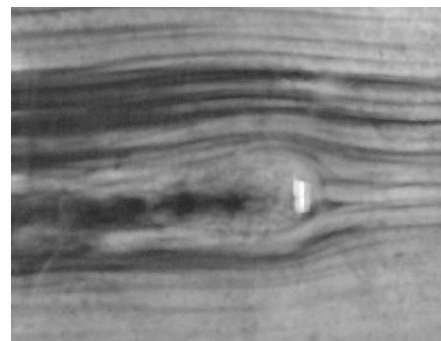
3) The mixing promoting efficiency of corrugated tab progressively increases with increase of NPR, whereas the maximum efficiency of plain tab is at correctly expanded state. In other words, the mixing efficiency of corrugated tab is appreciable at all levels of expansion, but for the plain tab the mixing efficiency is highest at the correctly expanded state. It may also be stated that corrugated tab is equally efficient in the presence of adverse, zero and favorable pressure gradients, whereas the plain tab is not.

4) The shock strength reduction caused by the corrugated tabs is found to be much higher than those caused by the plain tabs.

5) The mixing promoting small scale vortices generated by the corrugations are found to be responsible for the increased mixing efficiency of the corrugated tab.



a) Plain tab



b) Corrugated tab

Fig. 27 Water flow visualization pictures: a) plain tab, and b) corrugated tab.

## References

- [1] Ahuja, K. K., and Brown, W. H., "Shear Flow Control by Mechanical Tabs," AIAA Paper 89-0994, 1989.
- [2] Bohl, D., and Foss, J. F., "Enhancement of Passive Mixing Tabs by the Addition of Secondary Tabs," AIAA Paper 96-054, 1996.
- [3] Zaman, K. B. M. Q., Reeder, M. F., and Samimy, M., "Control of an Axisymmetric Jet Using Vortex Generators," *Physics of Fluids*, Vol. 6, 1994, pp. 778–793.  
doi:10.1063/1.868316.
- [4] Takama, Y., Suzuki, K., and Rathakrishnan, E., "Visualization and Size Measurement of Vortex Shed by Flat and Arc Plates in an Uniform Flow," *International Review of Aerospace Engineering (IREASE)*, Vol. 1, No. 1, Feb. 2008, pp. 55–60.
- [5] Thanigaarasu, S., Jayaprakash, S., Elangovan, S., and Rathakrishnan, E., "Influence of Tab Geometry and its Orientation on Underexpanded Sonic Jets," *Institution of Mechanical Engineers (UK), Part G, Journal of Aerospace Engineering*, Vol. 222, 2008, pp. 331–339.  
doi:10.1243/09544100JAERO299
- [6] Bradbury, L. J. S., and Khadem, A. H., "The Distortion of a Jet by Tabs," *Journal of Fluid Mechanics*, Vol. 70, No. 4, 1975, pp. 801–813.  
doi:10.1017/S0022112075002352
- [7] Zaman, K. B. M. Q., "Streamwise Vorticity Generation and Mixing Enhancement in Free Jets by Delta-Tabs," AIAA Paper 93-3253, 1993.
- [8] Wishart, D. P., Krothapalli, A., and Mungal, M. G., "Supersonic Jet Control Disturbances inside the Nozzle," *AIAA Journal*, Vol. 31, No. 7, 1993, pp. 1340–1341.  
doi:10.2514/3.11773
- [9] Reeder, M. F., and Samimy, M., "The Evolution of a Jet with Vortex-Generating Tabs: Real-Time Visualization and Quantitative Measurements," *Journal of Fluid Mechanics*, Vol. 311, 1996, pp. 73–118.  
doi:10.1017/S0022112096002510
- [10] Urban, W. D., Island, T. C., and Mungal, M. G., "Mixing Enhancement in Compressible Shear Layers Via Sub-Boundary Layer Disturbances," *Physics of Fluids*, Vol. 10, No. 4, 1998, pp. 1008–1020.  
doi:10.1063/1.869620.
- [11] Navinkumar, S., and Rathakrishnan, E., "Sonic Jet Control with Tabs," *Journal of Turbo and Jet Engines*, Vol. 19, Nos. 1–2, 2002, pp. 107–118.
- [12] Sreejith, R. B., and Rathakrishnan, E., "Cross-Wire as Passive Device for Supersonic Jet Control," AIAA Paper 2002-4052, 2002.
- [13] Lovaraju, P., Paparao, K. P. V., and Rathakrishnan, E., "Shifted Cross-Wire for Supersonic Jet Control," AIAA Paper 2004-4080, 2004.
- [14] Mrinal, K., Pankaj, S. T., and Rathakrishnan, E., "Studies on the Effect of Notches on Circular Sonic Jet Mixing," *Journal of Propulsion and Power*, Vol. 22, No. 1, 2006, pp. 211–214.  
doi:10.2514/1.8424
- [15] Ahuja, K. K., "Mixing Enhancement and Jet Noise Reduction Through Tabs Plus Ejectors," AIAA Paper 93-4347, 1993.
- [16] Carletti, M. J., Rogers, C. B., and Parekh, D. E., "Use of Streamwise Vorticity to Increase Mass Entrainment in a Cylindrical Ejector," *AIAA Journal*, Vol. 33, No. 9, 1995, pp. 1641–1645.  
doi:10.2514/3.12704
- [17] Grosch, C. E., Seiner, J. M., Hussaini, M. Y., and Jackson, T. L., "Numerical Simulation of Mixing Enhancement in a Hot Supersonic Jet," *Physics of Fluids*, Vol. 9, 1997, pp. 1125–1143.  
doi:10.1063/1.869203.
- [18] Steffen, C. J., Reddy, D. R., and Zaman, K. B. M. Q., "Numerical Modeling of Jet Entrainment for Nozzles Fitted with Delta Tabs," AIAA Paper 97-0709, 1997.
- [19] Rathakrishnan, E., "Experimental Studies on the Limiting Tab," *AIAA Journal*, AIAA, Reston, VA (to be published).
- [20] Rathakrishnan, E., *Instrumentation, Measurements, and Experiments in Fluids*, Taylor and Francis, Boca Raton, Florida, 2007.
- [21] Lovaraju, P., and Rathakrishnan, E., "Subsonic and Transonic Jet Control with Cross-Wire," *AIAA Journal*, Vol. 44, No. 11, Nov. 2006, pp. 2700–2705.  
doi:10.2514/1.17637
- [22] Rathakrishnan, E., *Gas Dynamics*, 2nd ed., Prentice Hall of India, New Delhi, India, 2008.
- [23] Rathakrishnan, E., "Waves in Correctly Expanded Supersonic Jets," *International Review of Aerospace Engineering (IREASE)*, Vol. 1, No. 6, Dec. 2008, pp. 536–538.
- [24] Verma, S. B., and Rathakrishnan, E., "Experimental Study on the Noise Characteristics of Notched Circular-Slot Jets," *Journal of Sound and Vibration*, Vol. 226, No. 2, 1999, pp. 383–396.  
doi:10.1006/jsvi.1999.2225

M. Glauser  
Associate Editor